Proceedings on Engineering Sciences

THEORETICAL STUDY OF HYDROMAGNETIC SQUEEZE FILM ROUGH TRUNCATED CONICAL PLATES WITH KOZENY-CARMAN MODEL BASED POROUS STRUCTURE

J. V. Adeshara
Hardik P. Patel[1]
G. M. Deheric
R. M. Patel

A B S T R A C T

Assuming that the surfaces of the truncated conical plates are transversely rough and considering the porous structure based on the Kozeny-Carman model, in the transverse magnetic field, the issue of the squeeze film between electrically conductive rough porous surfaces with electrically conductive lubricant is analyzed. The roughness of the surface of the bearing is dependent on a stochastic random variable with non-zero mean, variance and skewedness. After stochastically averaging the equation of Reynolds with regard to the parameter of random roughness, the pressure distribution, which in turn leads to the load carrying capacity, is solved with suitable boundary conditions. The analyses are displayed in both graphic and tabular form. It is known that the bearing roughness is transversely rough in general. Nonetheless, in the case of negative skewed roughness, the condition can be restored to some level by choosing the conductivities of the plate, if there is a negative variance. It is also found that even when there is no flow the magnetic field bearing can sustain a load.

1. INTRODUCTION

A variety of theoretical and experimental studies have been conducted on hydromagnetic lubrications for porous and flat metal bearings. In liquid metal lubrication, Elco and Huges (1962) analyzed magnetohydrodynamic pressure. The performance of magnetohydrodynamic squeeze films was studied by Kuzma (1964) and Kuzma, Maki and Donelly (1964). Shukla (1965) investigated the hydromagnetic theory of squeeze films in the presence of a transverse magnetic field to conduct lubricants between two non-conductive non-porous surfaces. The nature of hydromagnetic squeeze films between two non-porous surfaces was explored by Shukla and Prasad (1965) and the effect of surface conductivity on the performance of the bearing systems was studied. A number of theoretical and experimental studies were devoted to magnetohydrodynamic lubrication (Dodge, Osterle and Rauleau W.T., 1965), Maki, Kuzma and Donelly (1966);

---

[1] Corresponding author: R. M. Patel
Email: rmpatel2711@gmail.com

Snyder (1962)). Sinha and Gupta (1973, 1974) addressed the analysis of hydromagnetic effects on porous squeeze films in which annular plates and rectangular plates were considered. Patel and Hingu (1978) examined this impact among circular disks for squeeze films. Patel and Gupta (1979) used Morgan – Cameron approximation and simplified the analysis of hydromagnetic squeeze films for a number of geometric shapes between parallel plates. Patel (1975) studied the behavior of hydromagnetic films with tangential velocity slip between porous annular disks.

It is well established that the bearing surfaces create roughness after some run-in and wear. Many researchers analyzed the effect of surface roughness. (Davies (1963); Burton (1963); Tonder (1972); Michell (1950); Christensen and Tonder (1969a, 1969b, 1970). Tzeng and Saibel (1967); Berthe and Godet (1973). For both transverse and longitudinal surface roughness, Christensen and Tonder (1969a, 1969b, 1970). proposed an extensive general study. The approach of Christensen and Tonder was the basis of the analysis to investigate the effect of surface roughness in a number of (Ting (1975); Gupta and Deheri (1996); Prakash and Tiwari (1982); Guha (1993); Prajapati (1991, 1992); Andhari, Gupta and Deheri (1997, 1999). Patel and Deheri (2003, 2004) previously studied the performance of a magnetic fluid-based squeeze film between annular plates and circular and studied the impact of surface roughness on bearing system performance.

However, the increase in the conductivity of the plate results in improved performance (Prajapati (1995)) for circular plates, the transverse roughness of the bearing surfaces is shown to impact the performance of the system. Of course, the condition can be recovered to some degree particularly when negative variance arises in the case of negative skewed roughness.

The method adopted in the investigation of Patel and Deheri (2007) was modified and developed by Vadh et. al. (2010) to evaluate the adverse effect of transverse roughness for a magnetic fluid based squeeze film between rough porous conical plates. Patel et al (2018) discussed Ferrofluid squeeze film in rough conical plates Comparison of porous structures.

2. ANALYSIS

The geometry and configuration of the bearing system is shown in Figure: 1.

The lower plate with a porous face is supposed to be fixed while the upper plate moves towards the lower plate along its normal course. The plates are assumed to be electrically conductive and a lubricant fills the clearance gap between them. Between the plates there is a uniform transverse magnetic field.
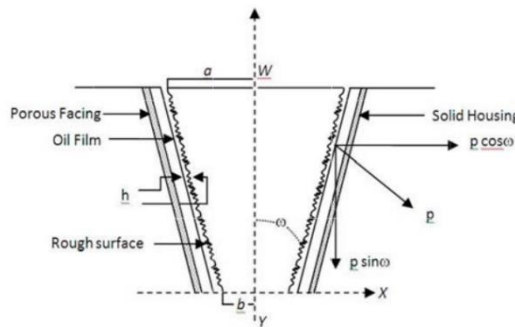

Figure 1. Bearing Structure

The flow in the porous medium obeys the modified form of Darcy's law. (Cf. Prajapati (1995), whereas the hydromagnetic lubrication theory equations hold in the film region. Following Tzeng and Saibel (1967) the film thickness h(x) is given by

$$h(x) = \bar{h}(x) + h_s(x)$$

If $\bar{h}(x)$ is the nominal film thickness between the mean bearing surface level and $h_s(x)$, the random deviation from the mean film thickness is determined by the probability density function f (h_s), - c $\leq h_s \leq$ c, C is the maximum h_s deviation. The mean α, the standard deviation σ and the parameter ε that is the symmetry measure of random variable h_s are defined by relationships.

$$\alpha = E(h_s)$$

$$\sigma^2 = E[(h_s - \alpha)^2]$$

and

$$\varepsilon = E[(h_s - \alpha)^3]$$

Where E refers to the expected value specified by E

$$E(R) = \int_{-c}^{c} R f(h_s) d h_s$$

The updated Reynolds equation for the lubricant film pressure is based on the normal hydromagnetic lubrication assumptions.

$$\frac{1}{x}\frac{d}{dx}\left(x\frac{dp}{dx}\right) = \frac{\dot{h}}{\left[\frac{2A}{\mu M^3}\left(\tanh\frac{M}{2}-\frac{M}{2}\right)-\frac{12\psi l_1 A}{\mu c^2}\right]} \bullet \frac{1}{\left[\frac{\phi_0+\phi_1+1}{\phi_0+\phi_1+\frac{\tanh(M/2)}{(M/2)}}\right]}$$

(1)

where A is the roughness term defined as

$$A = h^3 + 3h^2\alpha + 3h(\alpha^2+\sigma^2) + \varepsilon + 3\sigma^2\alpha + \alpha^3 + 12\psi l_1$$

and

$$M = B_0 h \left(\frac{s}{\mu} \right)^{1/2}$$

2.1 A Globular Sphere Model (GSM):

In this model, the porous material is packed with globular particles. The mean size of the particle is Dc.
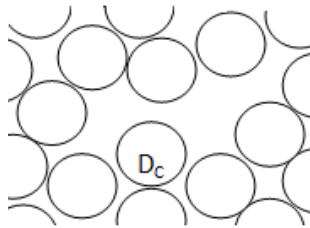

Figure 2. Structural model of porous sheets given by Kozeny – Carman

The Kozney – Carman terminology demonstrates that the permeability of the porous region takes shape.

$$\psi = \frac{D_c^2 e^3}{180(1-e)^2}$$

where e is the porosity.

Solving this equation with the use of boundary conditions.

$$p(a \, cosec\omega) = 0 \;\; ; \;\; p(b \, cosec\omega) = 0 \qquad (2)$$

Gives dimensional pressure distribution as

$$p = \frac{-\dot{h}\left(a^2 - b^2\right)cosec^2\omega \cdot \left[\frac{\ln(x/b cose\,c\,\omega)}{\ln(a/b)} - \frac{(xsin\,\omega/b)^2 - 1}{(a/b)^2 - 1} \right]}{4\left[\frac{2B}{M^3}\left(\tanh\frac{M}{2} - \frac{M}{2} \right) - \frac{\overline{\psi}e^3 B}{15(1-e)^2 c^2} \right]} \cdot \left[\frac{1}{\frac{\phi_0 + \phi_1 + 1}{\phi_0 + \phi_1 + \frac{\tanh(M/2)}{(M/2)}}} \right] \qquad (3)$$

where

$$B = 1 + 3\alpha^* + 3(\alpha^{*2} + \sigma^{*2}) + \varepsilon^* + 3\sigma^{*2}\alpha^* + \alpha^{*3}$$

and

$$\overline{\psi} = \frac{D_c^2 l_1}{h^3}$$

Then the load carrying capacity given by

$$w = 2\pi \int_{b cosec\omega}^{a cosec\omega} p \cdot x dx$$

is obtained in dimensionless form as

$$W = \frac{wh^3}{\mu \; \dot{h}\pi^2 \left(a^2 - b^2\right)^2 cos\,ec^2\omega}$$

$$= \frac{cosec^2\omega \cdot \left[\frac{(a/b)^2 + 1}{(a/b)^2 - 1} - \frac{1}{\ln(a/b)} \right]}{8\pi \left[\frac{2B}{M^3}\left(\tanh\frac{M}{2} - \frac{M}{2} \right) - \frac{\overline{\psi}e^3 B}{15(1-e)^2 c^2} \right]} \cdot \left[\frac{1}{\frac{\phi_0 + \phi_1 + 1}{\phi_0 + \phi_1 + \frac{\tanh(M/2)}{(M/2)}}} \right] \qquad (4)$$

3. RESULTS AND DISCUSSIONS

The distribution of pressure and the load carrying capacity depends on different parameters such as as $M, \psi, \phi_0 + \phi_1, \sigma^*, \varepsilon^*, \alpha^*, k, \omega$ and e in equation no.(3) and (4). The outcome of the squeeze film analyzed by Shukla and Prasad (1965) for non-porous smooth conducting plates can be obtained by taking into account the parameters of $\psi+$ and e = 0 and roughness parameters σ^*, α^* and ε^* are equal to zero. The results of Prakash and Vij (1973) are obtained for non-magnetic porous squeeze films in the limiting case when we take M=0 and the parameters of roughness $\sigma^* = \alpha^* = \varepsilon^* = 0$. Patel and Gupta (1979) results are obtained if ϕ_0 and ϕ_1 are taken as null.

It is also easy to see that $\phi_0 + \phi_1$ increases W for fixed values ψ, M, σ^*, α^* and ε^* k, ω and e .Although W decreases with higher fixed values Ψ and fix values $\phi_0 + \phi_1, \sigma^*, \alpha^*$ and ε^* k, ω and e. The impact of conductivity on the distribution of pressure comes by the factor

$$\left(\frac{\phi_0 + \phi_1 + \frac{\tanh(M/2)}{(M/2)}}{\phi_0 + \phi_1 + 1} \right)$$

For large values of M this tends to

$$\frac{\phi_0 + \phi_1}{\phi_0 + \phi_1 + 1}$$

as tanhM~ 1, 2 / M ~ 0. Both of these functions refer to the functions of $\phi_0 + \phi_1$. From a statistical point of view it is observed that the $\phi_0 + \phi_1$ load carrying capacity also increases as the pressure and the load rises.

Variation of load carrying capacity for different values of the magnetization parameter $M, \psi, \phi_0 + \phi_1, \sigma^*, \alpha^*, \varepsilon^*$ k, ω and e respectively is shown in Figures A1 – A8 (Appendix). From these figures one can see that the load carrying capacity increases considerably and also the negative skewed roughness tends to improve bearing system performance. Although the variance generally has a negative effect on the bearing system, the increase in the load carrying capacity is still sharp due to negative Avariance. The transverse surface roughness is clearly

seen to adversely affect the bearing system and the combined effect of the standard deviation and porosity is considerably negative.

Figures A9 – A15 (Appendix) show the load profile for different values with respect to $\phi_0 + \phi_1$ ψ, σ^*, α^*, ε^* k, ω and e. These figures show that the capacity of the load carrying increases considerably with respect $\phi_0 + \phi_1$. The variance has a very strong impact in increasing the capacity of the load carrying while the standard deviation has a nominal role. It can be noticed once again that the porosity has a considerably negative effect on the bearing system performance. From Figures A16 – A21 it can be concluded that the combined effect of the porosity and the transverse roughness parameters is significantly negative, while, In the case of negatively skewed roughness, the condition retrieves significantly, when it comes to negative variation. Figures A22 – A26 define the variability in load carrying capacity in terms of the combined effect of the roughness and porosity parameters. It is apparent that the combined effect of the parameters of roughness reduces the efficiency of the load carrying. (c. f. Figures A27 – A30) in Appendix. From figures A31 to A33, we can easily understand the load carrying capacity increases with increases with k, ω and e. In figures A34 and A35 LCC increases with reapect to e and ω And lastly in figure A36 load increases with respect to semi verticle angle.

Although the surface generally suffers due to roughness of the surface. This paper provides excellent scope for improving the efficiency of the bearing system, especially where there are adverse variances and this positive impact is further strengthened by combining the influence of the M magnetization parameter and the total electrical permeability. Although the porosity and standard deviation have an adverse effect for adverse skewed roughness with very small M values, the combined effect of the permeability and the adverse variance may be balanced.

Such debates indicate that the machine's life span may be increased in the case of rough bearings. By some of the figures it could be indicated that for both small and large values of M the bearing suffers when the plates are conducting electrically compared to the hydromagnetic case when the plates are non-conductive. This may possibly be because of fringing anomalies when the plates are electrically conducted. It is also obvious that the conductivity of the plates and the thickness of the plate increases the lubricant pressure and the capacity to carry the load.

This article makes it clear that variables of roughness must be taken into account when developing the bearing system, together with the option of M and permeability.

4. CONCLUSION

By choosing the plate conductivity and the magnetization parameter correctly, the negative effect induced by the transverse roughness can be compensated to some extent in the case of a negative skewed roughness. Furthermore, the observation that the rough bearing with magnetic field can support a load even if there is no flow gives this article ample scope in extending the bearing system's lifespan.

References:

Andhari, P., Gupta, J. L., & Deheri, G. M. (1999). Effect of transverse surface roughness on the behaviour of squeeze film in spherical bearing. *Journal of Applied Mechanical Engineering*, *4*, 19-24

Andhari, P., Gupta, J. L., & Deheri, G. M. (1997). Effect of longitudinal surface roughness on hydrodynamic lubrication of a slider bearings. *In proceeding of The Tenth International Conference on surface modification Technologies*, 872-880.

Berthe, D., & Godet, M. A. (1973). A more general form of Reynolds' equation –application of rough surfaces'. *Wear*, *27*, 345-357.

Burton, R. A. (1963). Effect of two-dimentional sinusoidal roughness on the load support charasticteristics of a lubricant film. *Transection ASME Journal of Basic Engineering*, *85*. 258-264.

Christensen, H., & Tonder, K. C. (1969a). Tribology of rough surface: Stochastic model of hydrodynamic lubrication. *SINTEF Report* No. 10/69-18.

Christensen, H. & Tonder, K. C. (1969b). Tribology of rough surface: Parametric study and comparison of lubrication models.*SINTEF Report* No. 22/69-18.

Christensen, H., & Tonder, K. C. (1970). The hydrodynamic lubrication of rough bearing surface of finite width. *ASME-ASLE Lubrication Conference*, Paper No.70- Lub-7.

Davis, M. G. (1963). The generation of pressure between rough lubricated, moving deformable surfaces. *Lubrication Engineering*, *19*, 246.

Dodge, F. T., Osterle, J. F., & Rouleau, W. T. (1965). Magnetohydrodynamic squeeze film bearings. *Journal of Basic engineering. Transactions of ASME*, *87*, 805-809.

Elco, R. A., & Huges, W. E. (1962). Magnetohydrodynamic pressurization in liquid metal lubrication'. *Wear*, *5*, 198-207.

Guha, S. K. (1993). Analysis of dynamic characteristics of hydrodynamic journal bearings with isotropic roughness effects. *Wear*, *167*, 173 -179.

Gupta, J. L., & Dahari G. M. (1996). Effect of roughness on the behaviour of squeeze film in a spherical bearing. *Tribology Transactions*, *39*, 99-102.

Kuzma, D. C., Maki, E. M., & Donnelly, R. J. (1964). The magnehydrodynamic squeeze films. *Journal of Fluid Mechanic*, *19*, 395-400.

Kuzma, D. C. (1964). Magnetohydrodynamic squeeze films. *Journal of Basic Engineering, Transactions of ASME*, 86, p. 441-444.

Maki., E. R., Kuzma, D. C., Donnelly, & R. J. (1966). Megnetohydrodynamic lubrication flow between parallel plates. *Journal of fluid mechanics*, *26*(3), 537-543.

Michell, A. G. (1950). *Lubrication, its principal and practice*. London: Blackie, p. 317.

Patel, K. C. (1975). Hydromagnetic squeeze film with slip velocity between two porous annular disks. *Transection of ASME, Journal of lubrication Technology*, *97*, 644. 647.

Patel, R. M., Deheri, G. M., & Vadh, P. (2018). Ferrofluid squeeze film in rough conical plates: *Comparison of porous structures. SCOPROS 2018*, *2*, 235-248.

Patel, R. M., & Deheri, G. M. (2000). Magnetic fluid based porous conical plates. *Industrial Lubrication and Tribology*, *59*(3), 143-147.

Patel, R. M., & Deheri, G. M. (2003). Magnetic fluidbased squeeze film behavior between rotating porous circular plates with a concentric circular pocket and surface roughness effects. *International Journal of Applied Mechanics and Engineering*, *8*(2), 271-277.

Patel, R. M., & Deheri, G. M. (2004). Magnetic fluid based squeeze film behavior between annular plates and surface roughness effect. *International Tribology Conference*, Rome, Italy, pp. 631-638.

Patel, K. C., & Gupta, J. L. (1979). Behaviour of hydromagnetic squeeze film between porous plates. *Wear*, *56*, 327-339.

Patel, K. C., & Hingu, J. V. Hydromagnetic squeeze film behaviour in porous circular disks. *Wear*, *49*, 239-246.

Prajapati, B. L. (1995). *On certain theoretical studies in hydrodynamics and elastohydrodynamics lubrication*, Dissertation, Ph. D. Thesis, S. P. University, V. V. Nagar.

Prajapati, B. L. (1991). Behaviour of squeeze film between rotating porous circular plates: surface roughness and elastic deformation effects. *Pure Applied Mathematical science*, *33*(1-2), 27-36.

Prajapati, B. L. (1992). Squeeze film behaviour between rotating porousn circular plates with concentric circular pocket: surface roughness and elastic deformation effects. *Wear*, *152*, 301-307.

Prakash, J., & Tiwari, K. (1982). Lubrication of porous bearing with surface corrugation. *J. Lubrication Technology, Transection ASME*, *104*, 127-134.

Prakash, J., & Vij, S. K. (1973). Load capacity and time height relations for squeeze film between porous plates'. *Wear, 24*, 309-322.

Shukla, J. B., & Prasad. R. (1965). Hydromagnetic squeeze films between two conducting surfaces. *Journal of Basic engineering, Transactions of ASME*, *87*. 818-822.

Shukla, J. B. (1978). Hydromagnetic theory of squeeze films. *ASME*, *87*, 142., 1965.

Sinha, P. C., & Gupta, J. L. (1973). Hydromagnetic squeeze films between porous rectangular plates. *Transection of ASME. Journal of lubrication technology.* Vol. 95. p.p. 394-398.

Sinha, P. C., & Gupta, J. L. (1974). Hydromagnetic squeeze films between porous annular disks. *Journal of Mathematical and Physical Sciences*, *8*, 413-422.

Snyder, W. T. (1962). Magnetohydrodynamic slider bearings. *Transection of ASME, Journal of Basic Engineering*, *85*, 429-434.

Ting, L. L. (1975). Engagement behavior of lubricated porous annular disks part I: Squeeze film phase surface roughness and elastic deformation effects. *Wear*, *34*, 159-182.

Tonder, K. C. (1972). Surface distributed waviness and roughness. *First World Conference in Industrial Tribology,* New Delhi, A3, pp.128.

Tzeng, S.T., & Saibel, E. (1967). Surface roughness effect on slider bearing lubrication. *Journal of Lubrication Technology, Transactions of ASME*, *10*, 334 -338.

Tzeng, S. T., & Saibel, E. (1967). Surface roughness effect on slider bearing lubrication, *Journal of Lubrication Technology, Transactions of ASME*, *10*. 334-338.

Vadh, P., Deheri, G. M., & Patel, R. M. (2010). Performance of hydromagnetic squeeze films between conducting porous rough conical plates. *MECCANICA*, *45*(6), 767-783.
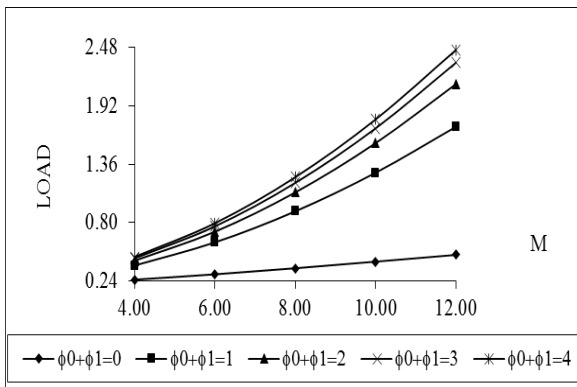
Appendix

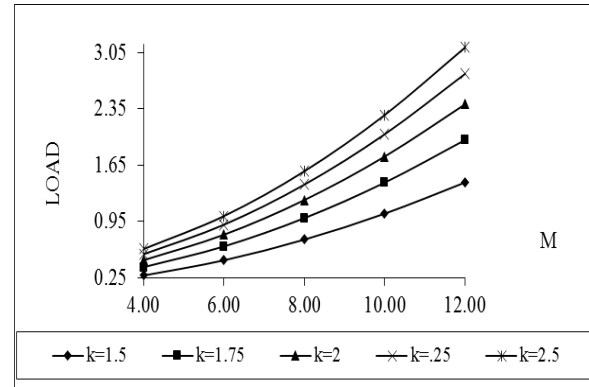**Figure A1.** Variation of load carrying capacity for M and $\phi_0 + \phi_1$
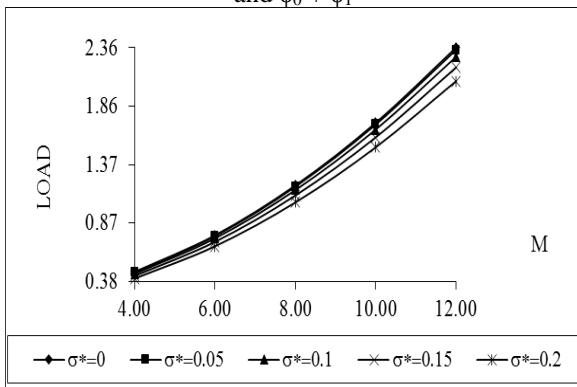

Figure A2. Distribution of load with respect to M and $\sigma*$

Figure A3. Variation of load bearing capacity for values of M and $\alpha*$

Figure A4. Variation of load with respect to M and $\varepsilon*$

Figure A5. Presentation of load capacity for M and k

Figure A6. Presentation of load capacity for M and ω

Figure A7. Presentation of load capacity for M and e
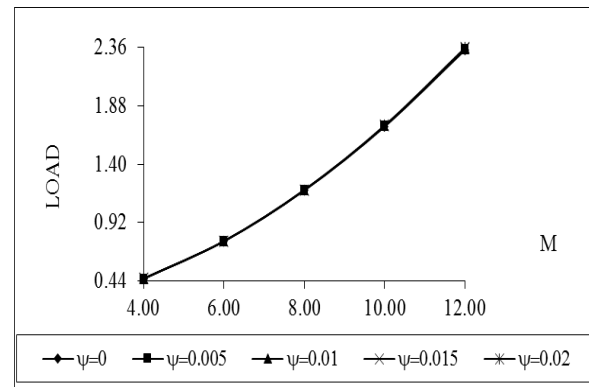
Figure A8. Presentation of load capacity for M and ψ
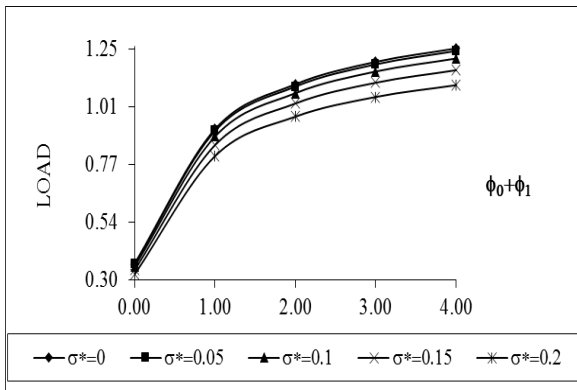
Figure A9. Variation of load carrying capacity for $\phi_0 + \phi_1$ and $\sigma*$
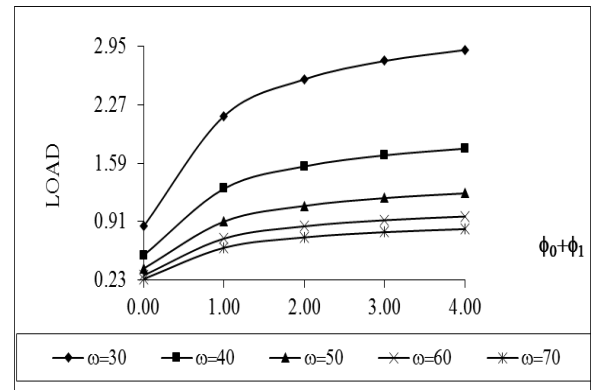
Figure A13. Variation of load with respect to $\phi_0 + \phi_1$ and ω
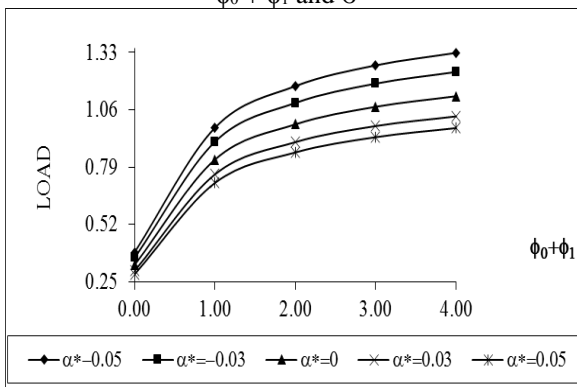
Figure A10. Distribution of load with respect to $\phi_0 + \phi_1$ and $\alpha*$
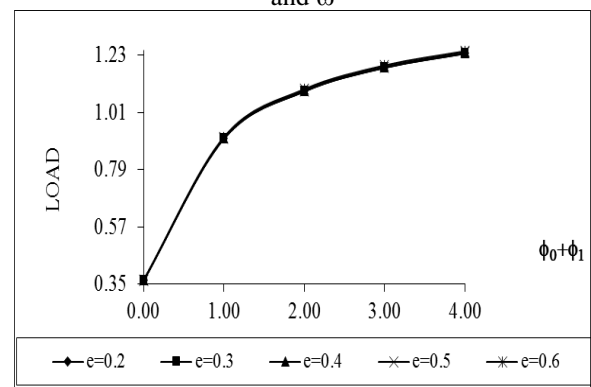
Figure: 14 Presentation of load capacity for $\phi_0 + \phi_1$ and e
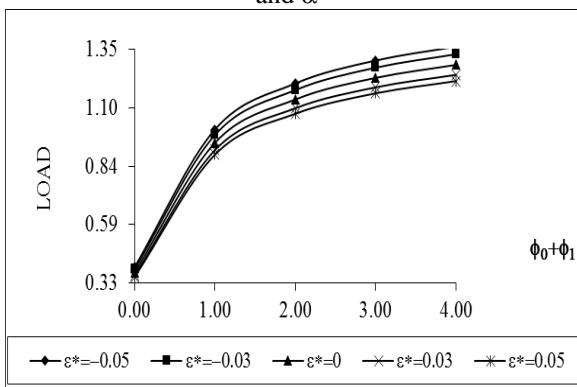
Figure A11. Profile of load bearing capacity for values of $\phi_0 + \phi_1$ and $\varepsilon*$
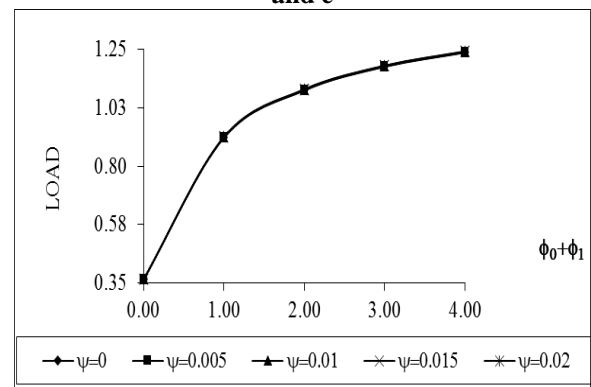
Figure A15. Variation of load with respect to $\phi_0 + \phi_1$ and ψ
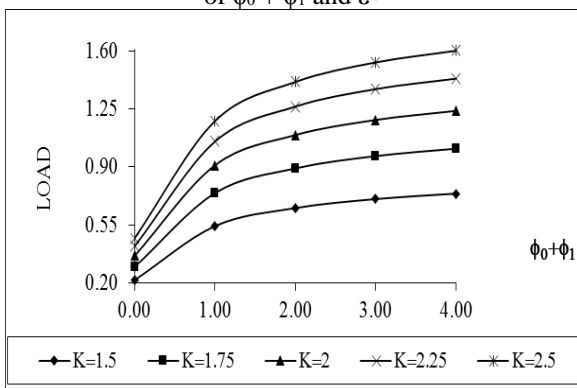
Figure A12. Variation of load with respect to $\phi_0 + \phi_1$ and k
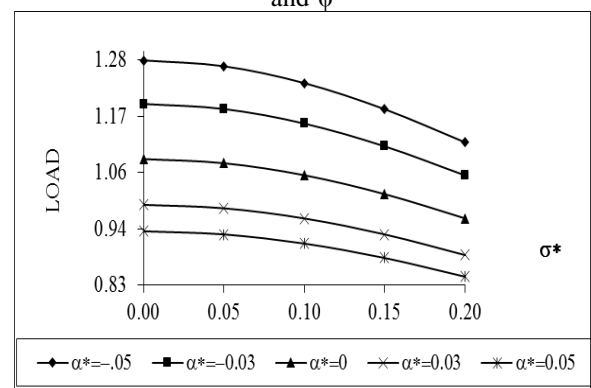
Figure A16. Variation of load carrying capacity for $\sigma*$ and $\alpha*$
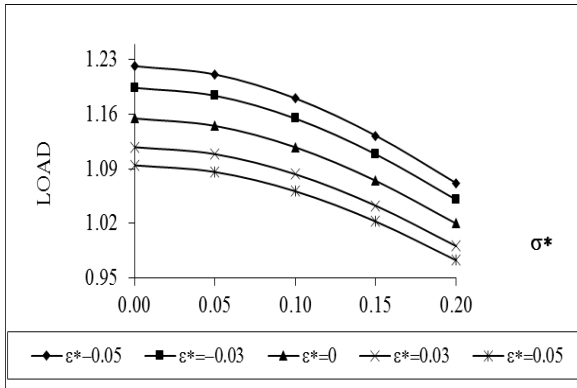
Figure A17. Variation of load with respect to $\sigma*$ and $\varepsilon*$

Figure A18. Variation of load with respect to $\sigma*$ and k

Figure A19. Variation of load with respect to $\sigma*$ and ω

Figure A20. Profile of load bearing capacity for values of $\sigma*$ and e

Figure A21. Profile of load bearing capacity for values of $\sigma*$ and ψ

Figure A22. Variation of load carrying capacity for $\alpha*$ and $\varepsilon*$

Figure A23. Variation of load with respect to $\alpha*$ and k
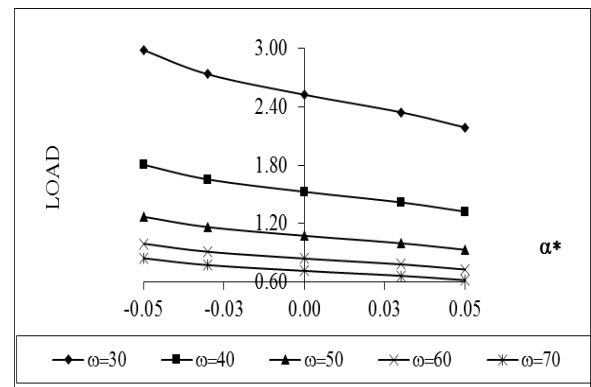
Figure A24. Variation of load with respect to $\alpha*$ and ω
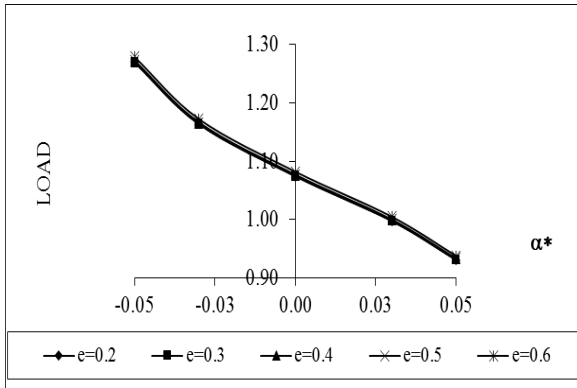
Figure A25. Profile of load bearing capacity for values of α∗ and e
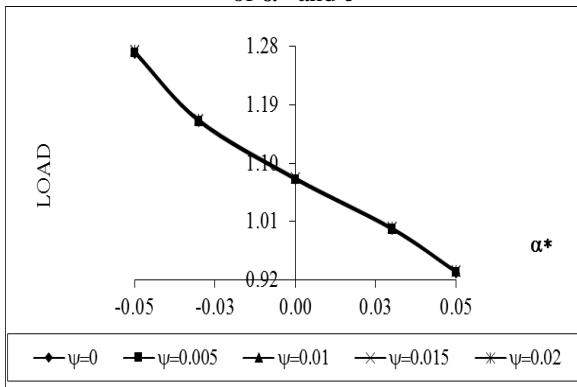

Figure A26. Variation of load with respect to α∗ and ψ

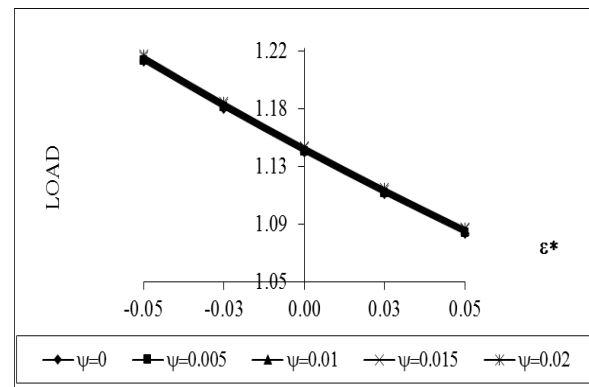**Figure A27.** Variation of load with respect to ε∗ and k

Figure A28. Variation of load with respect to ε∗ and ω
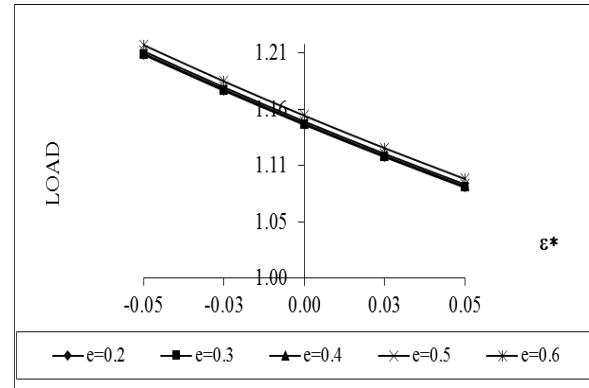
Figure A29. Variation of load with respect to ε∗ and e

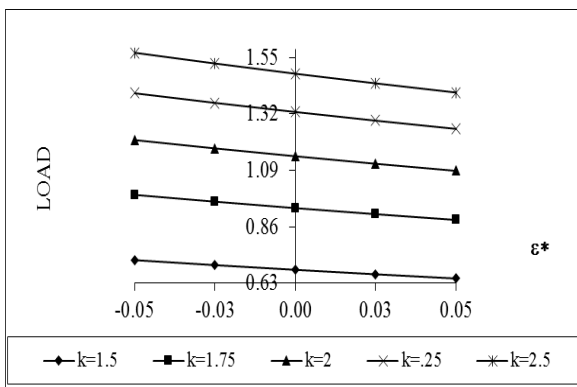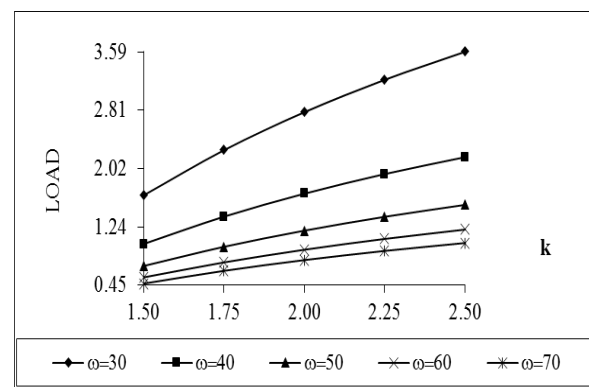**Figure A30.** Variation of load with respect to ε∗ and ψ

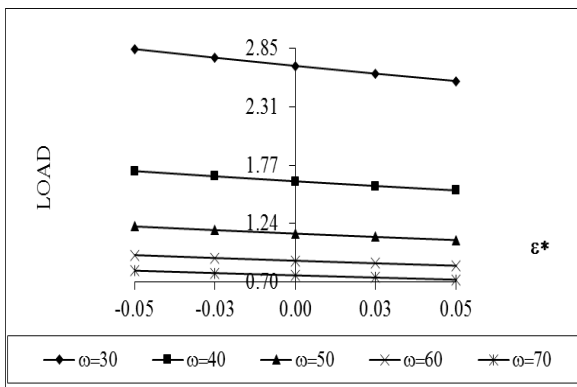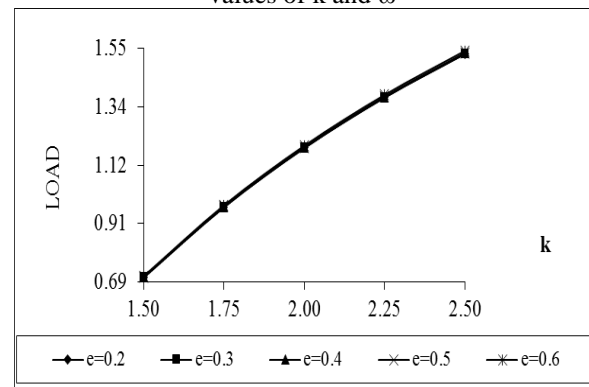**Figure A31.** Variation of load bearing capacity for values of k and ω

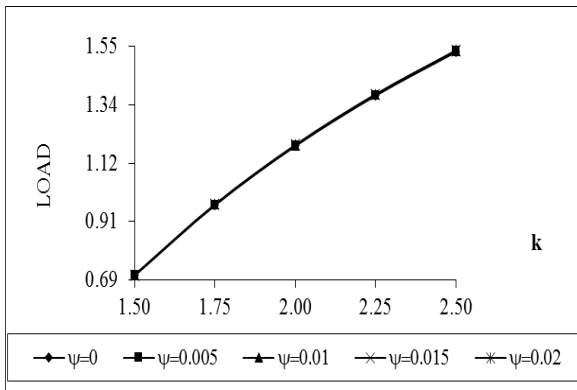**Figure A32.** Variation of load bearing capacity for values of k and e

Figure A33. Variation of load bearing capacity for values of k and ψ
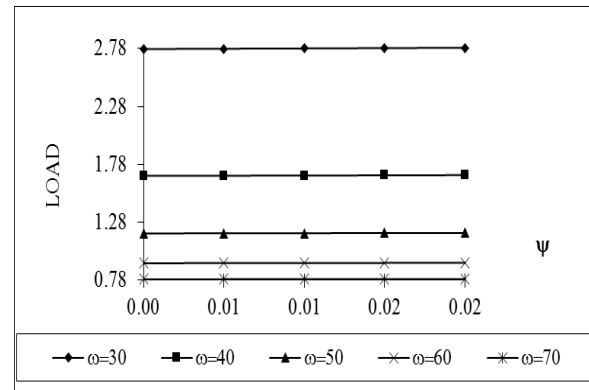

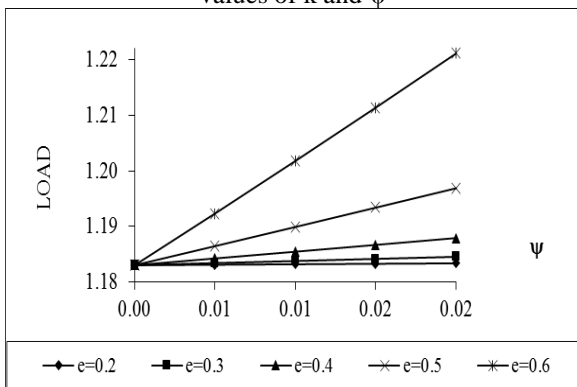**Figure A35.** Variation of load bearing capacity for values of ψ and ω

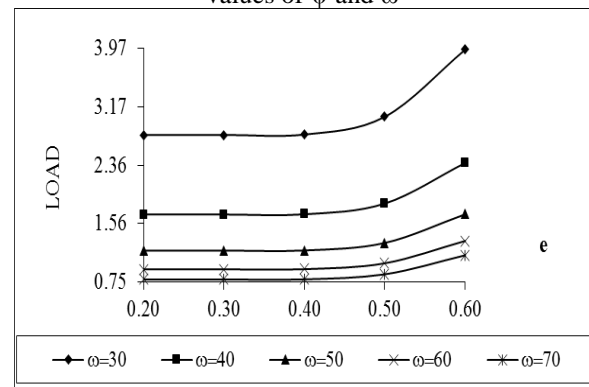**Figure A34.** Variation of load bearing capacity for values of ψ and e

Figure A36. Variation of load bearing capacity for values of e and ω

NOMENCLATURE

a	Radius of the plates (m)
H	Lubricant film thickness (m)
K	Permeability ($col^2 kgm/s^2$)
m	Porosity of the porous matrix
h'	$= dh/dt$ Squeeze velocity

$$M \quad = B_0 h \left(\frac{s}{\mu} \right)^{1/2} = \text{Hartmann number}$$

p   Pressure distribution (N/m^2)

$$P \quad \text{Non-dimensional pressure} = \frac{-ph^3}{\mu \dot{h} \pi a^2}$$

s   Electrical conductivity of the lubricant

w   Load carrying capacity (kgm/s^2)

W   Dimensionless load carrying capacity = $-\dfrac{wh^3}{\mu \dot{h} \pi^2 a^4}$

B_0 Uniform transverse magnetic field applied between the plates.

$$c^2 \quad = 1 + \frac{KM^2}{h^2 m}$$

h_0' Surface width of the lower plate (m)

h_1' Surface width of the upper plate (m)

s_0 Electrical conductivity of lower surface (mho)
s_1 Electrical conductivity of upper surface (mho)

$\phi_0(h)$ $= \dfrac{s_0 h_0'}{sh}$ = Electrical permeability of the lower surface

$\phi_1(h)$ $= \dfrac{s_1 h_1'}{sh}$ = Electrical permeability of the upper surface

ψ $= \dfrac{D_c^2 e^3}{180(1-e)^2}$ = Porosity

e	Eccentricity ratio
μ	Viscosity (kg/ms)f
σ*	Non-dimensional standard deviation (σ/h)
α*	Non-dimensional variance (α/h)
ε*	Non-dimensional skew ness ($ε/h^3$)
k	Aspect ratio
ω	Semi Vertical angel

J. V. Adeshara
Vishwakarma Government
Engineering College, Chandkheda,
Ahmedabad. - 382424 Gujarat State,
India.
adesharajatin01@gmail.com

Hardik P. Patel
Department of Humanity and Science,
L. J. Institute of Engineering and
Technology
Ahmedabad, Gujarat State India.
hardikanny82@gmail.com

G. M. Deheri
Department of Mathematics, S. P.
University, VallabhVidyanagar – 388
120, Gujarat State, India

R. M. Patel
Department of Mathematics, Gujarat
Arts and Science College,
Ahmedabad - 380 006 Gujarat State,
India. rmpatel2711@gmail.com